U.S. DEPARTMENT OF THE INTERIOR
U.S. GEOLOGICAL SURVEY

TO ACCOMPANY MAP
OPEN FILE REPORT 98-105

GEOLOGIC MAP OF THE STEMLER RIDGE QUADRANGLE, MALHEUR COUNTY, SOUTHEASTERN OREGON

By

By Jenda A. Johnson[1], Peter R. Hooper[2], Chris J. Hawkesworth[3], and G. Ben Binger[2]

[1] U.S. Geological Survey, Hawaiian Volcano Observatory, Hawai`i National Park, HI 96718; [2] Washington State University, Pullman, WA; [3] Open University, Milton Keynes, U.K. MK7 6AA

INTRODUCTION

The Stemler Ridge quadrangle was selected for a comprehensive geochemical study to expand our regional understanding of the relationship, if any, between north- and northwest-striking faults and stratigraphy. In addition, the thick sequence of basalt of Malheur Gorge may provide clues to an association between the coeval Columbia River Basalt Group to the north, and Steens Basalt to the south.

Geology was mapped on 1:24,000-scale topographic maps. Aerial photographs were used to interpret the extent of faults. Petrographic descriptions are based on field examination of hand samples. For additional mineralogic details, see Kittleman and others (1965) or Evans (1990).

Major and some trace element analyses were obtained using X-ray fluorescence spectroscopy (XRF) on fused glass beads on an automated Rigaku 3370 spectrometer at the GeoAnalytical Laboratory, Washington State University, Pullman, Washington. Analyses were conducted by Ben Binger and Diane Johnson (Hooper and others, 1993).

STRUCTURE

Normal faults are the dominant structural feature in the Stemler Ridge quadrangle. The faults occur chiefly in two discrete domains: northwest-striking normal faults prevail south of the Grasshopper Flat syncline, and north-striking normal faults are found to the north. The northwest-striking faults are the larger; their offset is at least 180 m, and strata deformed by them dip northeast. This pattern continues for 15 km south of the map area (Greene and others, 1972). The north-striking faults have offset less than 120 m, and beds dip uniformly west. No evidence was found for strike-slip faulting.

Grasshopper Flat occupies a west-trending asymmetric syncline (fig. 4). Strata on the north limb dip 12-20° southward, whereas the south limb dips 5-12°. The syncline changes eastward into a normal fault near Dishrag Canyon, with fault offset increasing to the east-southeast. Offset is 350 m near the east margin of the map and increases to 750 m 6 km east of the map area (Evans, 1990). The syncline and fault were buried by younger tuff and tuffaceous sedimentary deposits (Tyts) in middle and late Miocene time.

Extensive talus obscures all fault traces. Therefore, we have chosen to show no offset at fault intersections rather than guess at relative ages. Northwest- and north-striking faults may have been coeval or alternated over time. Synclinal folding appears to have predated the north-striking faults that disrupt the plateau north of Grasshopper Flat. East of the map area west-northwest-striking faults appear to be older (Evans, 1990).

The structure appears more complicated in Dishrag Canyon because units dip both west and south, draping the broad ridge directly north of Dishrag Spring. All older units exposed east of Dishrag Canyon form a monocline as they dip westward beneath the sedimentary strata of the older tuffaceous and sedimentary rocks (Tots) along the canyon floor. Older rocks exposed in eroded monoclines create irregular map contacts that at first glance suggest faulted relations (for example, see unit Thc in center of NW1/4 sec. 10, T. 20 S., R. 38 E.; also, see Dishrag Canyon on cross section A-A').

GEOLOGIC HISTORY

Miocene to Holocene tectonic and volcanic activity in eastern Oregon presumably occurred in response to east-west basin-and-range extension that began as early as Eocene time (Bennett, 1976; Zoback, 1989; Hooper and others, 1995; Morris and Hooper, 1997). The thick sequence of flows of the basalt of Malheur Gorge (Tm) were erupted across a broad area coeval with voluminous outpouring of Imnaha Basalt (earliest Columbia River Basalt Group strata) to the north and Steens Basalt to the south.

The Dinner Creek Ash-flow Tuff was deposited on a relatively flat surface above the basalt of Malheur Gorge as inferred from the uniform thickness and widespread distribution of this unit throughout most of the map area. The surface may have been part of a broad topographic low as suggested by Haddock (1967). The area underwent broad regional

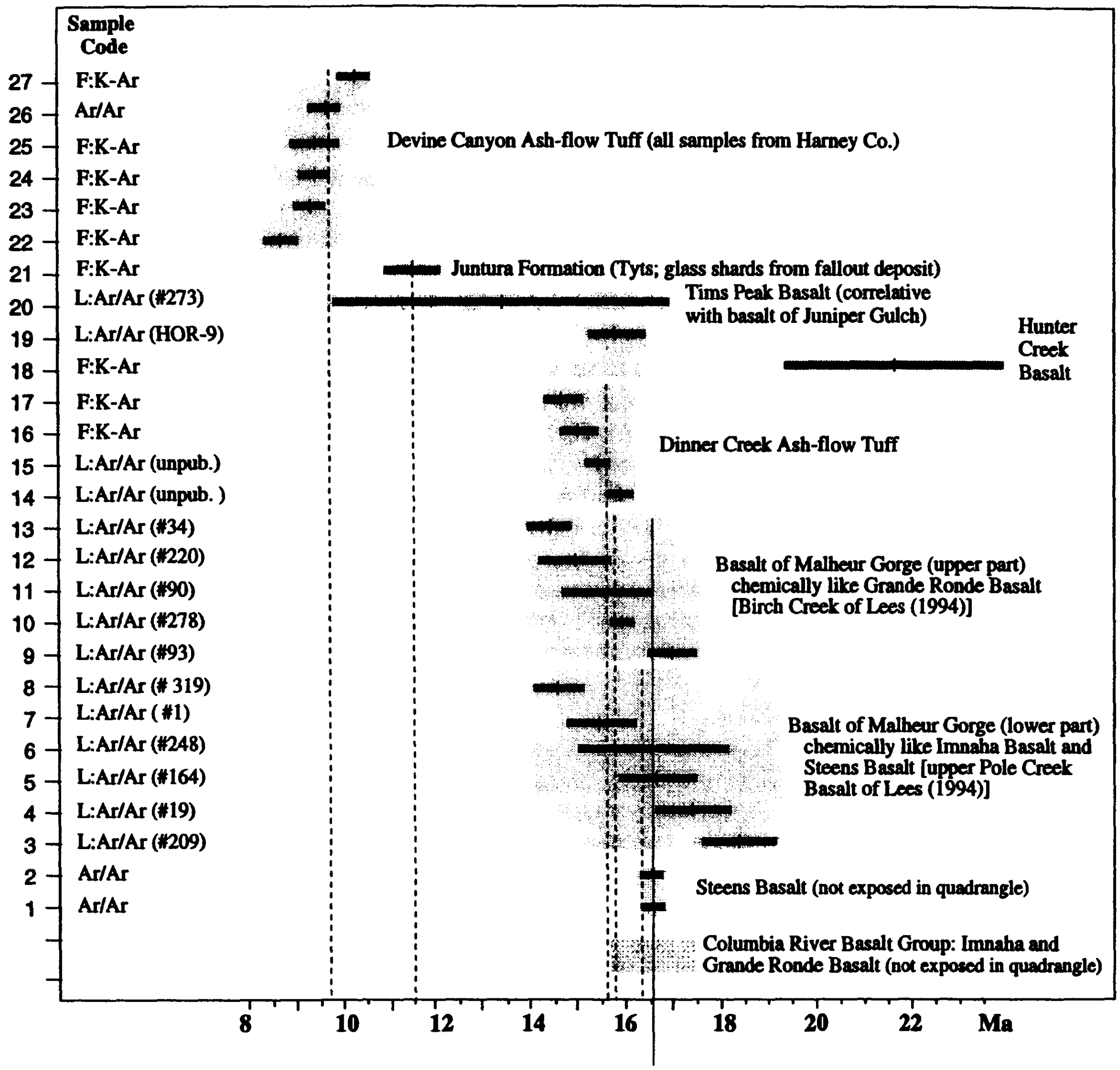

Figure 2: Isotopic ages for rock units exposed in the Stemler Ridge quadrangle showing age (+), relative error (horizontal bar), and weighted mean age (dashed vertical line). Weighted mean averages include both K-Ar and $^{40}Ar/^{39}Ar$, and do not account for the fact that recent $^{40}Ar/^{39}Ar$ ages are consistently older than early K-Ar ages. Pale shaded areas enclose multiple samples of single stratigraphic unit. Sample code refers to K-Ar and $^{40}Ar/^{39}Ar$ ages from Fiebelkorn and others (F; 1983) and Lees (L; 1994); sample number in parentheses. Steens Basalt ages from Swisher and others (1990); Devine Canyon Ash-flow Tuff $^{40}Ar/^{39}Ar$ age from Grunder and Deino (unpub. data, 1993). Ages for Hunter Creek Basalt do not fit the stratigraphic relations, so no best-fit line was added, and shaded area adjusted to match known stratigraphic relations. Field for Columbia River Basalt Group from Hooper and Conrey (1989).

subsidence, as indicated by the diatom-rich middle part of the older tuffaceous and sedimentary rocks (Haddock, 1967; this map). This unit thickens from 20 m in the southern part of the quadrangle to 140 m in the north and increases to over 200 m thick north of the map area (Haddock, 1967). Similar northward thickening occurs east of the map area in the Jonesboro quadrangle (Evans, 1990). To the north and northeast, the sedimentary sequence has not been mapped separately from the volcanic units (Brown and Thayer, 1966; Ferns and others, 1993), so the extent of the paleobasin cannot be determined. The sedimentary unit conformably overlies older strata, and the presence of diatomaceous sediment and clays indicates a low-energy depositional environment.

Palagonitic tuff cones interbedded in the sequence of older tuffaceous and sedimentary rocks north and east of the map area indicate that mafic eruptions continued during sedimentation there. In the map area vents of the intrusive pillow basalt (Tib) may have fed the basalt of Juniper Gulch, on the basis of compositional similarity and contact relations, which suggest that these flows invaded the soft, still-wet sediment.

There is no direct evidence for faulting prior to eruption of the basalt of Juniper Gulch. The basalt thickens in Juniper Gulch and west of the map area, but this may have resulted from prior structural relief, topographic relief, or local vent accumulations. Most of the faulting occurred following emplacement of the basalt of Juniper Gulch and before deposition of the younger tuff and tuffaceous sedimentary deposits (Tyts). As much as 100 m of the younger tuff and tuffaceous sedimentary deposits were deposited in the Grasshopper Flat-Calf Creek valley. Remnants of Devine Canyon Ash-flow Tuff and a compositionally similar unwelded ash that caps Tyts are inset into the Grasshopper Flat-Calf Creek valley, indicating that the tuff once filled the valley.

Devine Canyon Ash-flow Tuff and the younger tuff and tuffaceous sedimentary deposits (Tyts) were also deposited in fault-bounded valleys of the North Fork Malheur River ($W^1/2$ sec. 36, T. 20 S., R. 37 E.), Curry Canyon ($E^1/2$ sec. 8, T. 21 S., R. 38 E.), and Juniper Gulch (sec. 33, T. 20 S., R. 38 E.). In all three locations movement along northwest-striking faults continued after emplacement of the younger tuff and tuffaceous sedimentary deposits. A small outcrop of Devine Canyon Ash-flow Tuff and younger tuff and tuffaceous sedimentary deposits was also found in upper Cave Canyon, indicating the canyon was already more than 240 m deep prior to 10 Ma.

The most recent eruption in the map area produced the basalt of Cave Creek. Its age is known only as younger than the basalt of Juniper Gulch because it fills the canyon cut in the basalt. Its vent location has not been found.

The paleo-Malheur River wound through fault-bounded valleys roughly parallel to its current course. Possible evidence for existence of the river before emplacement of the Devine Canyon Ash-flow Tuff is a cobble deposit (QTs) of reworked Dinner Creek Ash-flow Tuff and basalt lying 180 m above the valley floor. A sedimentary deposit (Qs_1) 90 m above the valley floor contains cobbles of Devine Canyon Ash-flow Tuff.

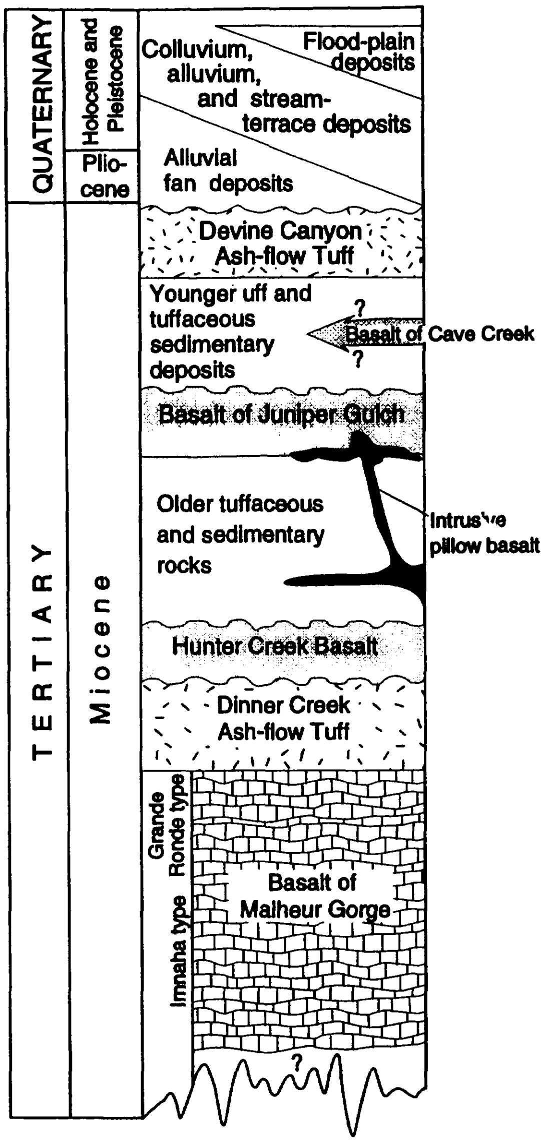

Figure 1: Stratigraphic units exposed in Stemler Ridge quadrangle

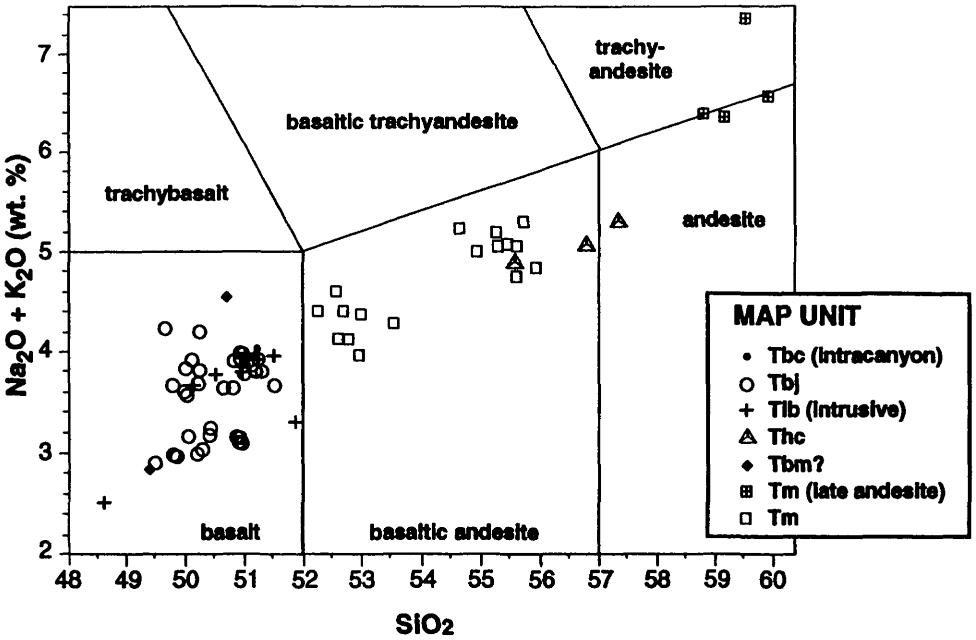

Figure 3: Chemical analyses of basalt and andesite in the Stemler Ridge quadrangle plotted on a total alkali-silica diagram (Le Bas and Streckeisen, 1991.) Data from table 1.

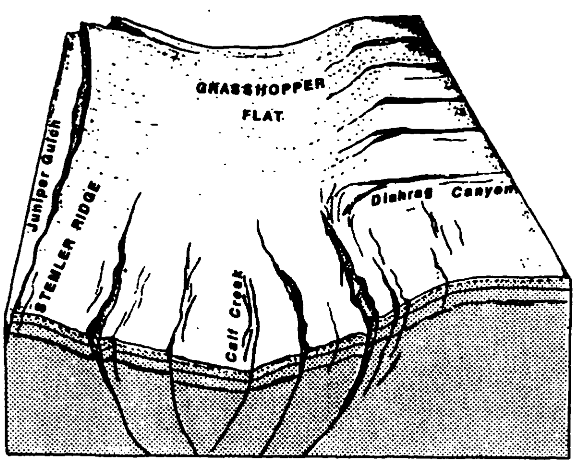

Figure 4: Cartoon view of Grasshopper Flat from east edge of map area. Depicts structural features present prior to deposition of the valley-filling unit of younger tuff and tuffaceous sedimentary deposits

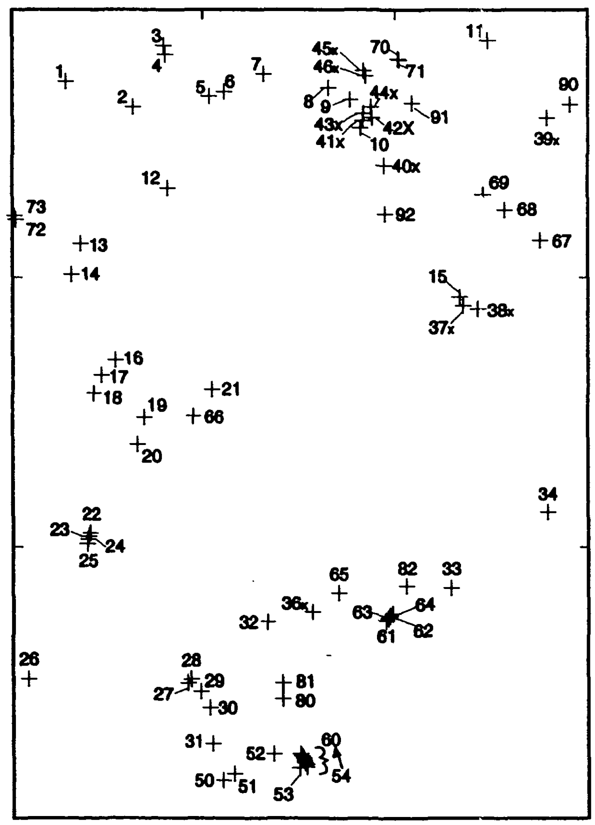

Figure 5: Index map showing locations for samples analyzed in table 1. See map sheet for precise locations

References Cited

Bennett, E.H., 1976, Reconnaissance geology and geochemistry of the South Mountain-Juniper Mountain region, Owyhee County, Idaho: Idaho Bureau of Mines and Geology Pamphlet 166, 80 p.

Binger, G.B., 1997, The volcanic stratigraphy of the Juntura region, eastern Oregon: Pullman, Washington State University, M.S. thesis, 206 p.

Brown, C.E., and Thayer, T.P., 1966, Geologic map of the Canyon City quadrangle, northeastern Oregon: U.S. Geological Survey Miscellaneous Geologic Investigations Map I-477, scale 1:250,000.

Evans, J.G., 1990, Geologic map of the Jonesboro quadrangle, Malheur County, Oregon: Oregon Department of Geology and Mineral Industries Geological Map Series GMS-66, scale 1:24,000.

Evans, J.G., and Binger, G.B., 1997, Geologic map of the Westfall Butte quadrangle, Malheur County, Oregon: U.S. Geological Survey Open-file report, OF 97-481 scale 1:24,000.

Ferns, M.L., Brooks, H.C., Evans, J.G., and Cummings, M.L., 1993, Geologic map of the Vale 30- x 60-minute quadrangle, Malheur County, Oregon, and Owyhee County, Idaho: Oregon Department of Geology and Mineral Industries Geological Map Series GMS-77, scale 1:100,000.

Fiebelkorn, R.B., Walker, G.W., MacLeod, N.S., McKee, E.H., and Smith, J.G., 1983, Index to K-Ar age determinations for the state of Oregon: Isochron/West, no. 37, p. 3-60.

Greene, R.C., 1973, Petrology of the welded tuff of Devine Canyon, southeastern Oregon: U.S. Geological Survey Professional Paper 797, 26 p.

Greene, R.C., Walker, G.W., and Corcoran, R.E., 1972, Geologic map of the Burns quadrangle, Oregon: U.S. Geological Survey Miscellaneous Geologic Investigations Map I-680, scale 1:250,000.

Haddock, G.H., 1967, The Dinner Creek Ash-flow Tuff of the Malheur Gorge area, Malheur County, Oregon: Eugene, University of Oregon, Ph.D. dissertation, 110 p.

Hooper, P.R., Bailey, D.G., McCarley-Holder, G.A., 1995, Tertiary calc-alkaline magmatism associated with lithospheric extension in the Pacific Northwest: Journal of Geophysical Research, v. 100, 10,303-10,319.

Hooper, P.R. and Conrey, R.M., 1989, A model for the tectonic setting of the Columbia River Basalt eruptions: Geological Society of America Special Paper 239, p. I659-I668.

Hooper, P.R., Johnson, D.M., and Conrey, R.M., 1993, Major and trace-element analyses of rocks and minerals by automated X-ray spectrometry: Washington State University, Department of Geology, Open-file Report, 38 p.

Johnson, J.A., 1994, Geologic map of the Krumbo Reservoir quadrangle, Harney County, southeastern Oregon: U.S. Geological Survey Miscellaneous Field Studies Map MF-2267, scale 1:24,000.

——1995, Geologic evolution of the Duck Creek Butte eruptive center, High Lava Plains, southeastern Oregon: Corvallis, Oregon State University, M.S. thesis, 151 p.

——1996, Geologic map of the Page Springs quadrangle, Harney County, southeastern Oregon: U.S. Geological Survey Open-file Report, OF97-675, scale 1:24,000.

Johnson, J.A., Binger, G.B., Hooper, P.R., and Hawkesworth, C.J., 1996, Implications of structure and stratigraphy in the Juntura area, east-central Oregon [abs.]: Geological Society of America Cordilleran Section, v. 28, no. 5, p. 78.

Kittleman, L.R., Green, A.R., Haddock, G.H., Hagood, A.R., Johnson, A.M., McMurray, J.M., Russell, R.G., and Weeden, D.A., 1967, Geologic map of the Owyhee region, Malheur County, Oregon: University of Oregon Museum of Natural History Bulletin 8, scale 1:125,000.

Kittleman, L.R., Green, A.R., Hagood, A.R., Johnson, A.M., McMurray, J.M., Russell, R.G., and Weeden, D.A., 1965, Cenozoic stratigraphy of the Owyhee region, southeastern Oregon: University of Oregon Museum of Natural History Bulletin 1, 45 p.

Lawrence, R.D., 1976, Strike-slip faulting terminates the Basin and Range province in Oregon: Geological Society of America Bulletin, v. 87, p. 846-850.

Lees, K.R., 1994, Magmatic and tectonic changes through time in the Neogene volcanic rocks of the Vale area, Oregon, northwestern U.S.A.: Milton Keynes, United Kingdom, Open University, Ph.D. dissertation, 284 p.

Le Bas, M.J., Le Maitre, R.W., Streckeisen, A., and Zenettin, B., 1986, A chemical classification of volcanic rocks based on the total alkali-silica diagram: Journal of Petrology, v. 27, p. 745-750.

Morris, G.A., and Hooper, P.R., 1997, Petrogenesis of the Colville igneous complex, northeast Washington: Implications for Eocene tectonics in the northern U.S. Cordillera: Geology, v. 25, no. 9, p. 831-834.

Sherrod, D.R., and Johnson, J.A., 1994, Geologic map of the Irish Lake quadrangle, U.S. Geological Survey Miscellaneous Field Studies Map, MF-2256, scale 1:24,000.

Stimac, J.P., and Weldon, R.J., II, 1992, Paleomagnetism and tectonic rotations of the Rattlesnake and Devine Canyon Ash-flow Tuffs, northern Basin and Range, southern Oregon [abs.]: Geological Society of America Abstracts with Programs, v. 24, no. 5, p. 83.

Shotwell, J.A., 1963, Pliocene mammalian communities of the Juntura Basin *in* Shotwell, J.A.,ed., 1963, The Juntura Basin: Studies in earth history and paleoecology: American Philosophical Society Transactions, v. 53, 77 p.

Swisher, C.C., Ach, J.A., and Hart, W.K., 1990, Laser fusion $^{40}Ar/^{39}Ar$ dating of the type Steens Mountain Basalt, southeastern Oregon, and the age of the Steens geomagnetic polarity transition [abs.]: Eos (American Geophysical Union Transactions), v. 71, no. 43, p. 1,296.

Zoback, M.L., 1989, State of stress and modern deformation of the northern Basin and Range province: Journal of Geophysical Research, v. 94, p. 7,105-7,128.

LIST OF TABLES

LIST OF FIGURES

PLATE

Table 1: Whole-rock compositions for Stemler Ridge samples, grouped by map unit

	Basalt of Juniper Gulch (Tbj)																				
Map #	**1**	**2**	**3**	**4**	**5**	**6**	**7**	**8**	**9**	**10**	**11**	**12**	**13**	**14**	**15**	**16**	**17**	**18**	**19**	**20**	**21**
Map unit	**Tbj**	**Tbj**	**Tbj**	**Tbj**	**Tbj**	**Tbj**	**Tbj**	**Tbj**	**Tbj**	**Tbj**	**Tbj**	**Tbj**	**Tbj**	**Tbj**	**Tbj**	**Tbj**	**Tbj**	**Tbj**	**Tbj**	**Tbj**	**Tbj**
SiO_2	50.80	50.85	49.79	50.64	50.90	50.96	50.30	50.40	50.94	50.81	50.05	51.49	50.99	50.12	50.95	49.66	50.23	51.29	50.41	50.01	50.91
Al_2O_3	17.50	17.59	19.38	17.60	18.01	17.72	17.41	17.64	17.97	17.14	17.21	18.36	17.63	18.21	17.49	19.39	19.56	16.71	17.50	18.42	17.18
TiO_2	1.02	0.84	1.05	1.16	0.84	0.82	0.81	0.85	0.86	1.27	0.83	1.18	1.15	1.31	1.19	1.21	1.21	1.35	1.09	1.23	1.27
FeO*	9.00	8.93	9.34	9.19	8.36	8.46	8.79	9.04	8.89	8.84	8.90	9.07	8.80	9.77	9.05	9.55	8.98	9.59	8.87	9.98	9.46
MnO	0.16	0.14	0.16	0.15	0.17	0.21	0.15	0.16	0.15	0.16	0.18	0.12	0.17	0.16	0.14	0.16	0.16	0.16	0.15	0.20	0.16
CaO	10.39	10.78	10.77	10.21	11.37	11.69	11.15	11.28	11.16	10.00	11.28	10.40	10.11	10.08	10.20	10.02	10.39	9.95	11.36	9.82	9.77
MgO	7.21	7.51	5.52	7.08	7.08	6.86	8.16	7.20	6.74	7.50	8.21	5.39	7.04	6.03	6.64	5.38	5.24	6.77	7.15	6.14	6.90
K_2O	0.73	0.53	0.59	0.63	0.46	0.50	0.45	0.47	0.46	0.88	0.42	0.63	0.69	0.64	0.87	0.72	0.64	0.77	0.44	0.67	0.77
Na_2O	2.91	2.62	3.08	3.00	2.63	2.58	2.59	2.77	2.68	3.03	2.74	3.04	3.08	3.28	3.12	3.51	3.17	3.04	2.73	3.15	3.21
P_2O_5	0.29	0.19	0.33	0.33	0.19	0.19	0.19	0.20	0.16	0.37	0.18	0.32	0.33	0.38	0.34	0.40	0.41	0.38	0.29	0.37	0.37
Trace elements (ppm)																					
Ni	136	138	113	138	132	141	146	130	119	117	130	129	122	125	116	106	108	112	104	132	128
Cr	218	327	143	235	278	342	300	298	293	217	272	267	223	140	224	64	74	221	191	83	240
Sc	32	32	34	30	36	36	36	33	30	33	33	32	32	33	30	29	28	33	44	31	29
V	246	236	240	258	247	251	230	231	262	258	238	268	255	277	246	260	271	274	258	242	274
Ba	338	242	324	350	313	632	217	228	303	334	304	1011	371	487	360	475	1191	558	616	879	536
Rb	8	7	5	6	6	8	5	5	7	9	5	7	7	6	8	7	8	7	5	6	9
Sr	415	319	442	437	333	366	320	323	326	427	322	493	437	497	447	542	530	440	366	500	458
Zr	89	69	87	90	66	68	65	67	67	97	66	94	89	92	91	101	98	102	78	103	99
Y	23	30	24	22	26	21	21	21	19	23	21	25	25	23	20	24	25	24	24	25	23
Nb	7	4	6	6	4	4	3	5	4	8	6	8	7	7	8	7	8	8	5.1	7.7	8
Ga	15	17	18	19	16	17	17	19	20	18	17	18	20	16	20	20	21	20	16	16	19
Cu	70	99	99	82	67	112	67	122	87	86	100	77	60	82	55	76	88	76	36	90	67
Zn	72	59	74	77	65	67	62	67	62	79	59	84	80	89	81	80	83	80	72	92	80
Pb	0	2	1	0	0	0	2	2	0	0	0	0	2	1	0	0	3	2	0	2	1
Th	0	0	0	4	0	4	0	0	1	0	2	0	0	0	1	1	3	0	6	23	2
La	0	11	8	11	12	1	0	0	0	5	0	3	0	4	6	14	13	12	8	42	11
Ce	0	0	0	0	85	59	49	50	51	81	47	44	47	35	27	40	38	40	0	2	51

Major-element data normalized to 100%. *Total iron is expressed as FeO. "†" denotes values >120% of highest standard.
Data are from Diane Johnson and Ben Binger, GeoAnalytical Laboratory, Washington State University, Pullman WA.

[Table 1-p.1]

(Table 1 cont.)

(Unit Tbj, cont)													Intrusive basalt (Tib) Ventiagglomerate, dikes, sills, and pillow basalt of unit Tots						
Map #	22	23	24	25	26	27	28	29	30	31	32	33	34	36x	37x	38x	39x	40x	41x
Map unit	Tbj	Tbj	Tbj	Tbj	Tbj	Tbj	Tbj	Tbj	Tbj	Tbj	Tbj	Tbj	Tbj	Tib	Tib	Tib	Tib	Tib	Tib
SiO2	49.97	50.91	49.84	49.51	50.21	51.20	50.04	51.09	49.78	50.21	51.24	51.16	50.23	48.62	51.49	51.17	51.23	50.11	50.94
Al2O3	18.07	17.24	17.58	17.36	17.49	17.06	17.42	16.84	17.40	17.75	17.55	17.32	19.27	18.09	17.31	17.27	17.13	16.64	17.13
TiO2	1.10	1.26	0.96	0.94	1.13	1.27	1.08	1.27	0.97	0.78	1.23	1.31	1.32	0.99	1.32	1.32	1.29	1.29	1.26
FeO*	9.23	9.58	8.92	8.71	9.51	9.93	9.36	9.68	9.26	8.39	9.10	9.35	9.58	9.20	9.04	8.76	8.93	9.66	9.58
MnO	0.15	0.16	0.17	0.16	0.16	0.15	0.16	0.16	0.17	0.16	0.19	0.15	0.15	0.17	0.14	0.14	0.16	0.15	0.16
CaO	10.62	9.78	11.35	11.62	10.38	9.91	10.46	9.72	11.24	11.38	9.99	9.86	10.01	11.81	10.02	10.37	9.86	9.81	10.00
MgO	6.90	6.79	8.00	8.57	7.07	6.31	7.56	7.03	8.00	8.17	6.41	6.62	4.78	8.32	6.32	6.61	7.08	8.32	6.72
K2O	0.60	0.79	0.38	0.38	0.67	0.70	0.64	0.75	0.39	0.38	0.75	0.88	0.75	0.28	0.87	0.91	0.95	0.77	0.79
Na2O	3.00	3.14	2.57	2.51	3.01	3.11	2.92	3.13	2.59	2.60	3.18	2.99	3.45	2.23	3.10	3.07	2.98	2.89	3.06
P2O5	0.35	0.36	0.23	0.23	0.36	0.36	0.35	0.34	0.22	0.18	0.36	0.38	0.45	0.30	0.39	0.38	0.38	0.38	0.37
Trace elements (ppm)																			
Ni	150	139	124	135	142	129	154	141	134	156	130	128	86	136	123	139	134	197	109
Cr	172	217	239	256	178	218	173	223	237	349	232	207	66	257	210	232	216	292	215
Sc	36	25	33	37	30	28	34	30	36	34	32	33	29	38	34	26	34	29	35
V	259	253	252	238	255	252	254	253	248	236	246	263	284	261	265	266	260	253	268
Ba	340	430	239	205	299	664	373	451	402	283	701	368	1247	154	374	427	365	310	350
Rb	4	8	2	5	7	8	6	9	4	4	7	8	7	3	11	16	11	7	9
Sr	423	455	283	277	403	482	424	460	298	310	449	441	570	274	450	466	440	442	435
Zr	88	98	67	67	90	101	90	102	72	61	94	98	106	68	101	102	97	94	98
Y	24	26	23	22	22	26	22	28	23	21	24	23	26	24	22	22	22	22	23
Nb	7	8	4	4	7	7.5	6.1	7.0	3.5	3	7	8	8	5	7	7	8	6	7
Ga	19	20	16	12	17	16	17	17	17	18	16	18	16	18	19	18	19	21	21
Cu	75	42	82	81	54	72	55	87	93	115	78	84	75	69	86	86	82	80	86
Zn	75	81	61	63	79	87	79	83	63	64	85	79	93	64	81	84	81	82	80
Pb	0	0	0	1	0	4	4	0	1	0	2	1	2	0	0	0	3	2	3
Th	0	0	0	1	0	15	0	21	0	0	4	0	3	1	2	4	0	0	0
La	5	0	16	9	7	44	39	26	31	0	22	13	20	0	2	4	7	5	3
Ce	82	102	89	89	52	1	1	2	3	51	53	0	67	25	102	45	26	68	89

[Table 1-p.2]

(Table 1 cont.)

	(unit Tib, cont.)					Basalt of Malheur Gorge (Tm)														
Map #	42x	43x	44x	45x	46x	50	51	52	53	54	55	56	57	58	59	60	61	62	63	64
Map unit	Tib	Tib	Tib	Tib	Tib	Tm	Tm	Tm	Tm	Tm	Tm	Tm	Tm	Tm	Tm	Tm	Tm	Tm	Tm	Tm
SiO_2	51.06	50.49	51.00	51.87	50.98	48.88	59.50	52.97	53.54	52.77	52.25	55.70	55.23	55.90	54.61	55.58	52.58	55.58	54.90	55.27
Al_2O_3	17.44	17.70	17.08	16.96	16.97	17.03	15.74	14.98	15.27	14.65	14.78	13.79	13.50	13.83	13.46	13.85	15.14	13.88	13.83	13.79
TiO_2	1.27	1.16	1.26	1.05	1.25	1.12	2.78	1.83	1.93	1.77	1.89	2.34	2.32	2.25	2.52	2.20	1.80	2.26	2.50	2.21
FeO*	8.68	9.33	9.48	8.51	9.26	9.76	8.33	10.05	9.71	10.64	11.13	11.22	12.17	11.31	12.73	11.40	11.05	11.37	12.13	12.00
MnO	0.15	0.15	0.16	0.14	0.17	0.17	0.10	0.24	0.21	0.18	0.18	0.19	0.19	0.20	0.20	0.19	0.19	0.18	0.18	0.19
CaO	10.01	10.31	9.76	10.29	9.92	11.15	4.45	9.80	10.00	9.68	9.27	7.40	7.30	7.62	7.35	7.46	9.48	7.78	7.60	7.23
MgO	7.16	6.74	6.95	7.67	7.31	8.43	1.18	5.49	4.74	5.91	5.77	3.69	3.69	3.67	3.51	3.91	5.37	3.80	3.44	3.91
K_2O	0.83	0.73	0.87	0.57	0.84	0.34	3.44	0.97	0.86	0.82	0.97	1.82	1.82	1.62	1.82	1.62	0.80	1.44	1.58	1.52
Na_2O	3.03	3.04	3.09	2.73	2.95	2.96	3.92	3.40	3.42	3.31	3.43	3.47	3.38	3.23	3.40	3.43	3.32	3.32	3.42	3.54
P_2O_5	0.37	0.34	0.36	0.21	0.36	0.16	0.55	0.28	0.31	0.27	0.32	0.39	0.40	0.37	0.41	0.35	0.28	0.38	0.42	0.35
Trace elements (ppm)																				
Ni	121	133	113	138	127	122	4	37	28	44	37	11	9	6	15	4	47	11	13	0
Cr	223	253	213	262	216	248	15	160	157	149	142	16	14	16	24	16	103	20	20	11
Sc	40	40	31	32	37	36	34	30	34	40	40	33	35	31	35	36	41	36	41	39
V	269	254	243	240	252	247	420	367	380	356	313	344	336	332	367	348	326	324	379	356
Ba	315	359	345	229	338	142	887	431	485	392	400	597	588	582	598	599	397	565	584	575
Rb	7	7	11	6	8	7	131	17	25	16	17	44	43	43	44	36	14	35	37	38
Sr	426	440	427	349	423	244	361	409	411	401	382	317	321	338	306	336	402	333	305	321
Zr	96	91	97	76	96	79	241	135	139	134	145	206	207	200	223	194	132	197	216	196
Y	23	22	23	21	23	19	†47	32	33	32	32	42	42	41	†46	40	30	39	†47	39
Nb	7	7	8	5	7	7.1	21.5	8	8	7.5	7.6	15.9	16.0	15.0	16.4	14.2	9.2	15.8	17.1	15.2
Ga	18	18	20	15	17	20	27	22	22	21	23	24	24	25	22	25	22	22	21	23
Cu	81	52	79	85	85	73	6	150	157	†153	131	75	73	71	104	36	86	70	106	39
Zn	79	79	83	72	80	71	†146	96	101	96	100	†127	†125	†120	†131	†122	96	117	†126	†122
Pb	0	0	1	2	0	0	8	6	2	4	5	7	9	8	9	6	2	5	7	6
Th	1	0	1	2	0	0	31	2	0	6	23	26	25	19	24	29	1	20	26	12
La	17	0	17	15	12	21	82	11	0	36	42	67	48	60	57	55	30	57	71	42
Ce	91	108	99	89	84	1	9	34	48	1	2	4	4	4	5	6	4	6	7	6

[Table 1-p.3]

(Table 1 cont.)

(Unit Tm, cont.)													Intracyn	Din.Crk.	
										Hunter	Creek	Basalt	basalt	Tuff	Ash
Map #	65	66	67	68	69	70	71	72	73	80	81	82	90	91	92
	Tm	Tm	Tm	Tm	Tm	Tm	Tm	Tm?	Tm?	Thc	Thc	Thc	Tbc	Tdc	Tyts
SiO2	55.45	59.15	52.55	52.68	52.95	58.80	59.87	50.71	49.37	56.75	55.56	57.32	51.20	76.92	74.79
Al2O3	13.68	13.66	15.15	14.90	15.70	13.66	14.20	19.27	17.85	13.64	13.29	14.01	16.97	11.55	12.38
TiO2	2.35	1.82	1.96	1.82	1.81	1.88	2.01	1.38	0.77	2.38	2.30	2.43	1.32	0.15	0.30
FeO*	11.68	10.69	10.23	10.38	9.56	10.92	8.66	9.49	9.04	11.33	13.04	9.82	8.55	2.94	3.25
MnO	0.18	0.21	0.19	0.23	0.15	0.22	0.21	0.15	0.18	0.18	0.20	0.19	0.06	0.01	0.07
CaO	7.49	5.36	9.24	9.71	9.84	5.42	5.54	9.62	11.74	7.00	6.99	7.16	10.20	0.32	0.59
MgO	3.72	2.01	5.76	5.60	5.74	1.93	2.08	4.34	8.06	3.19	3.26	3.29	7.35	0.22	0.31
K2O	1.73	2.46	1.03	0.98	0.69	2.61	2.83	0.90	0.28	1.97	1.85	2.04	0.98	3.56	5.42
Na2O	3.34	3.89	3.57	3.42	3.28	3.77	3.73	3.64	2.56	3.11	3.07	3.27	3.06	4.30	2.85
P2O5	0.40	0.74	0.33	0.28	0.28	0.70	0.89	0.50	0.15	0.45	0.44	0.47	0.38	0.03	0.03
Trace elements (ppm)															
Ni	9	0	43	36	49	0	0	75	139	0	0	4	132	17	22
Cr	19	21	148	159	114	13	11	62	208	13	15	31	197	8	13
Sc	36	25	30	32	26	20	25	26	38	32	32	30	28	3	2
V	341	48	332	346	350	57	58	282	218	354	372	386	253	11	14
Ba	630	962	450	427	401	933	1103	487	265	810	719	944	361	1326	305
Rb	44	63	20	17	11	64	67	8	2	49	44	55	9	74	130
Sr	324	317	361	401	412	315	346	589	260	343	320	350	437	35	42
Zr	204	254	142	134	128	247	255	118	57	211	202	213	99	364	
Y	42	57	32	31	29	57	59	25	25	†45	43	45	21	75	131
Nb	16.8	19	8	7	7	19	19	8	3	16.9	17.0	19	8	25	
Ga	19	24	21	23	18	26	25	17	15	27	24	25	16	23	31
Cu	77	0	131	148	111	2	2	122	113	1	0	4	86	2	7
Zn	†123	148	102	98	98	145	149	92	60	†141	†133	138	84	133	198
Pb	6	8	4	0	2	7	8	0	1	8	10	6	4	13	30
Th	21	7	3	0	2	7	6	3	1	26	31	7	1	8	12
La	64	27	8	16	0	34	27	6	23	61	54	11	11	35	96
Ce	6	99	66	50	48	150	133	1	1	7	7	16	33	152	275

[Table 1-p.4]

Table 2: Latitude, longitude, and township (south) and range (east) for XRF-analysis locations in Table 1 and Figure 5

Map #	Map unit	latitude	longitude	sec., T and R	Map #	Map unit	latitude	longitude	sec., T and R
1	Tbj	43.8640	118.1133	sec 1, T20, R37	40x	Tib	43.8508	118.0440	sec 10, T20, R38
2	Tbj	43.8600	118.0985	sec 6, T20, R38	41x	Tib	43.8578	118.0487	sec 3, T20, R38
3	Tbj	43.8695	118.0918	sec 31, T10, R38	42x	Tib	43.8583	118.0467	sec 3, T20, R38
4	Tbj	43.8682	118.0915	sec 31, T10, R38	43x	Tib	43.8590	118.0483	sec 3, T20, R38
5	Tbj	43.8617	118.0820	sec 5, T20, R38	44x	Tib	43.8600	118.0468	sec 3, T20, R38
6	Tbj	43.8623	118.0787	sec 5, T20, R38	45x	Tib	43.8648	118.0480	sec 3, T20, R38
7	Tbj	43.8652	118.0700	sec 5, T20, R38	46x	Tib	43.8657	118.0483	sec 34, T19, R38
8	Tbj	43.8630	118.0560	sec 4, T20, R38	50	Tm	43.7558	118.0792	sec 17, T21, R38
9	Tbj	43.8612	118.0512	sec 4, T20, R38	51	Tm	43.7568	118.0767	sec 17, T21, R38
10	Tbj	43.8567	118.0492	sec 3, T20, R38	52	Tm	43.7598	118.0678	sec 9, T21, R38
11	Tbj	43.8703	118.0215	sec 35, T19, R38	53	Tm	43.7577	118.0625	sec 9, T21, R38
12	Tbj	43.8473	118.0910	sec 7, T20, R38	54	Tm	43.7578	118.0610	sec 9, T21, R38
13	Tbj	43.8387	118.1102	sec 12, T20, R37	55	Tm	43.7582	118.0610	sec 9, T21, R38
14	Tbj	43.8338	118.1122	sec 13, T20, R37	56	Tm	43.7585	118.0613	sec 9, T21, R38
15	Tbj	43.8303	118.0275	sec 14, T20, R38	57	Tm	43.7588	118.0615	sec 9, T21, R38
16	Tbj	43.8207	118.1025	sec 19, T20, R38	58	Tm	43.7592	118.0617	sec 9, T21, R38
17	Tbj	43.8183	118.1057	sec 19, T20, R38	59	Tm	43.7595	118.0618	sec 9, T21, R38
18	Tbj	43.8155	118.1073	sec 19, T20, R38	60	Tm	43.7598	118.0622	sec 9, T21, R38
19	Tbj	43.8118	118.0960	sec 19, T20, R38	61	Tm	43.7803	118.0437	sec 34, T20, R38
20	Tbj	43.8075	118.0977	sec 30, T20, R38	62	Tm	43.7807	118.0432	sec 34, T20, R38
21	Tbj	43.8162	118.0815	sec 20, T20, R38	63	Tm	43.7810	118.0428	sec 34, T20, R38
22	Tbj	43.7938	118.1082	sec 25, T20, R37	64	Tm	43.7813	118.0423	sec 34, T20, R38
23	Tbj	43.7933	118.1085	sec 36, T20, R37	65	Tm	43.7847	118.0538	sec 33, T20, R38
24	Tbj	43.7928	118.1087	sec 36, T20, R37	66	Tm	43.8120	118.0855	sec 20, T20, R38
25	Tbj	43.7922	118.1088	sec 36, T20, R37	67	Tm	43.8392	118.0105	sec 11, T20, R38
26	Tbj	43.7713	118.1217	sec 12, T21, R37	68	Tm	43.8440	118.0180	sec 11, T20, R38
27	Tbj	43.7708	118.0868	sec 8, T21, R38	69	Tm	43.8463	118.0225	sec 11, T20, R38
28	Tbj	43.7713	118.0862	sec 8, T21, R38	70	Tm	43.8675	118.0410	sec 34, T19, R38
29	Tbj	43.7695	118.0840	sec 8, T21, R38	71	Tm	43.8673	118.0408	sec 34, T19, R38
30	Tbj	43.7670	118.0820	sec 8, T21, R38	72	Tm?	43.8410	118.1250	sec 12, T20, R37
31	Tbj	43.7615	118.0813	sec 8, T21, R38	73	Tm?	43.8408	118.1250	sec 12, T20, R37
32	Tbj	43.7802	118.0693	sec 33, T20, R38	80	Thc	43.7683	118.0660	sec 9, T21, R38
33	Tbj	43.7853	118.0293	sec 25, T20, R38	81	Thc	43.7708	118.0660	sec 9, T21, R38
34	Tbj	43.7970	118.0087	sec 35, T20, R38	82	Thc	43.7857	118.0392	sec 34, T20, R38
36x	Tib	43.7817	118.0597	sec 33, T20, R38	90	Tbc			sec 1, T20, R38
37x	Tib	43.8290	118.0268	sec 14, T20, R38	91	Tdc	43.8607	118.0380	sec 3, T20, R38
38x	Tib	43.8285	118.0237	sec 14, T20, R38	92	Ash (Tdv?)	43.8433	118.0438	sec 10, T20, R38
39x	Tib	43.8583	118.0090	sec 1, T20, R38					